Embrace EU project

Milestone MS4

Prepared by F. Guichard, worked done in collaboration with F. Couvreux and C. Taylor

Identification of different regimes of triggering as function of surface and atmospheric conditions

This work focuses on daytime deep convective triggering over land, and makes use of several datasets documenting a relatively flat Sahelian area, enclosed within (10°W, 10°E) and (10°N,20°N) during the monsoon season (June-July-August, September). More than 2000 cases were identified by Taylor et al. (2011) over the period 2006 to 2010 with satellite data. Figure 1 shows the location of these different cases. As expected, convective initiations are found to be relatively more numerous in the vicinity of topographic features (orange dots). However, they only account for a limited number of cases (compare grey and black bars in Fig. 2).

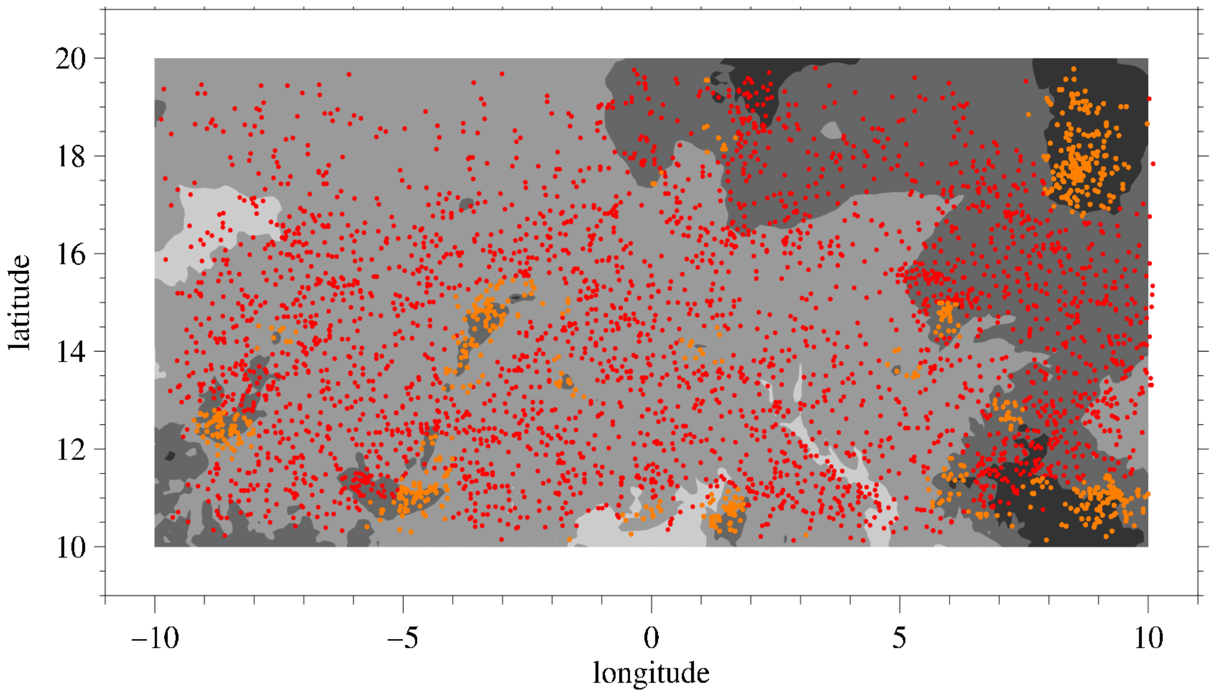

Figure 1 *: Location of the set of identified convective initiation cases during the months of June to September of the years 2006 to 2010. Each dot stands for one case and orange dots indicate initiation that possibly involve an influence of orography. Orography is shown with grey shading (with 200m between iso-shades).*

More than 300 cases are found within each latitude band between 11°N and 17°N (Fig. 2, upper panel). The smaller number of cases south of 11°N is possibly due to the heavier cloud cover prevailing there preventing the identification of numerous cases. On the other hand, north of 17°N, the smaller number of cases likely reflects true climatological features, i.e. convective initiations being less numerous within this northern, more arid, fringe of the domain. Figure 2 lower panel indicates a maximum of cases in the early afternoon, around 15h. This is somehow earlier than reported by previous studies (e.g. Machado et al 2002) and likely due to differences in the employed methodology. Indeed, the time of initiation of deep convective events refers here to the very first cloudy developments, prior to convection becoming very deep.

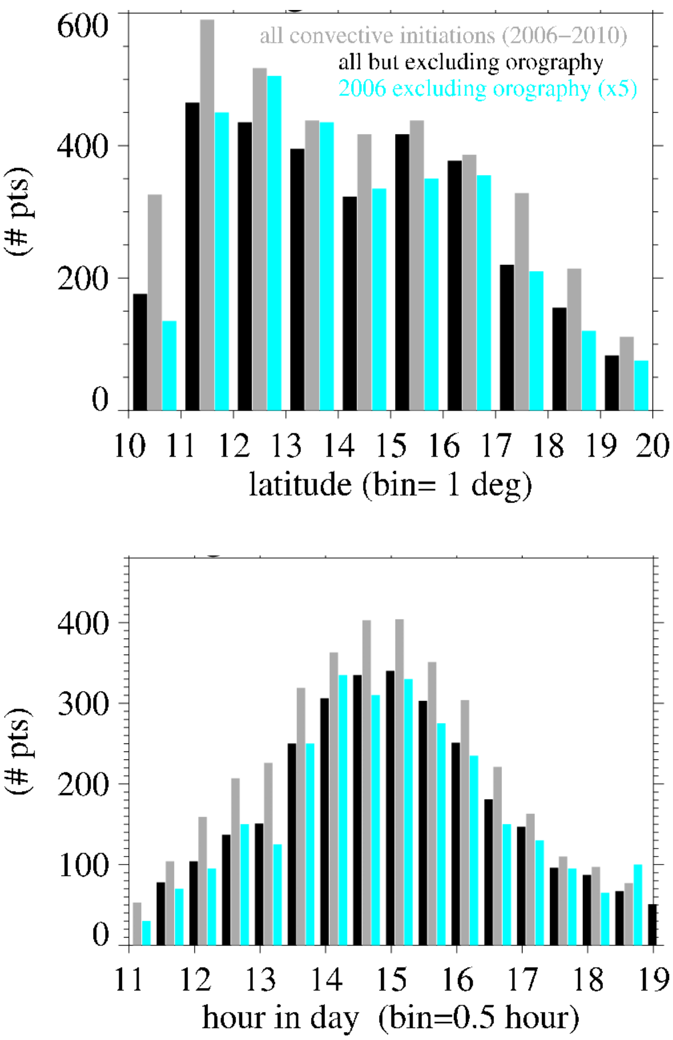

***Figure 2** : histograms of the number of cases as a function of latitude (upper panel) and hour in day (lower panel); all cases (grey bars), cases over flat terrain only (black bars) and for 2006 only (cyan bars).*

Finally, Figure 2 illustrates that the cases sampled in 2006 are well representative of the results obtained for the 5-year period and the subsequent work focuses on this year only, because more extended datasets are available for this AMMA SOP year (Lebel et al. 2010).

Information on the atmospheric environment has been obtained from meteorological analyses. This is illustrated in Figure 3 which also stresses that daytime initiation of deep convection arises within a very wide range of atmospheric conditions. For information, the characteristics of two cases that have been studied in details is indicated with disks (see legend). It turned out that initiation of deep convection is observed even under fairly unfavourable environment conditions (notably high height of the level of free convection located some 100 mb higher than the boundary layer top at 12h). This figure indicates that these unfavourable situations are also frequently characterized by high heights of the lifting condensation level, located only slightly below the level of free convection. In other words, 1D considerations suggests that once moist convection is initiated, it is more likely to become deep than if the difference between the lifting condensation level and the level of free convection was stronger.

Information on the surface conditions has been inferred from the satellite datasets used in Taylor et al. (2011), and also from off-line land surface simulations performed with ISBA using realistic inputs, in particular rainfall, with a time step of 30 min and 0.5° x 0.5° spatial resolution (cf

ALMIP project, Boone et al. 2009). The main interest of these simulations it that they provide information on surface fluxes, beyond the characterization of surface soil moisture and temperature inferred from satellite observations. This is illustrated with evaporative fraction in Fig. 4 which again, emphasizes the wide range of surface conditions under which deep convection is triggered. If splitting the range of evaporative fraction into four equal intervals between 0 and 1, one finds about the same number of cases within each interval.

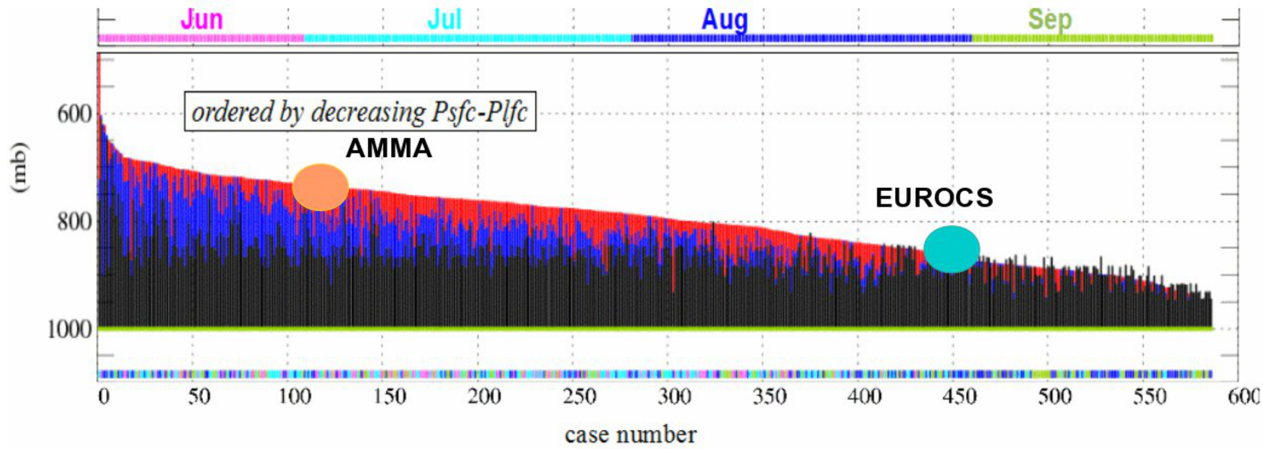

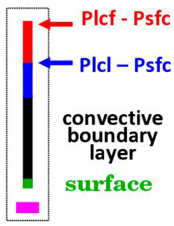

Figure 3 *: Level of free convection (top of red bar), lifting condensation level (top of blue bar) and convective boundary layer height (top of black bar) at 12h for the cases sampled in 2006. The three variables are expressed in as pressure height departures from surface pressure and computed with vertical profiles extracted from the ECMWF analysis at the closest point to initiation. The cases are ordered by decreasing level of free convection. The colour line below indicates the month during which the initiation occurred. The level of free convection corresponding to cases of daytime deep convection studied in Couvreux et al (2012) [AMMA] and Guichard et al. (2004) [EUROCS] are indicated with orange and cyan disks.Plfc: level of free convection. Plcl: lifting condensation level, Psfc: surface pressure.*

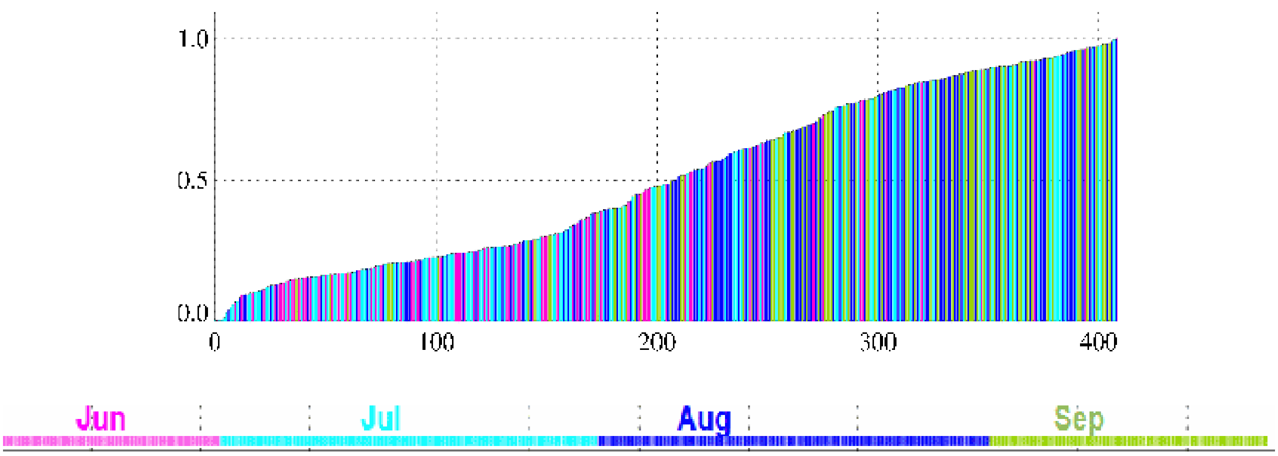

Figure 4 *: Evaporative fraction (EF, unitless) for 2006 cases estimated fom ISBA offline runs (ALMIP project, Boone et al. 2009). The cases are ordered by increasing EF and the colour of the bar below indicates the month during which the initiation occurred. (note than less cases are presented here because the information was missing for some cases).*

The mean surface and atmospheric conditions are not independent and couplings between them have been identified with independent datasets (analyses and satellite data). This is illustrated in Fig. 5. The lifting condensation level is found to regularly decrease as the surface becomes wetter, which is consistent with cooler and moister (in terms of specific humidity) conditions encountered over wetter soils. The daytime increase of the lifting condensation level is also stronger dry soil, which is expected from considerations on the partition of surface sensible and latent heat flux and boundary layer growth. This daytime increase is nevertheless observed over the whole range of soil moisture. On the other hand, only for soil moisture values higher than 10% ($m/^3.m^3$) does the level of free convection decreases from 6h to 12h.

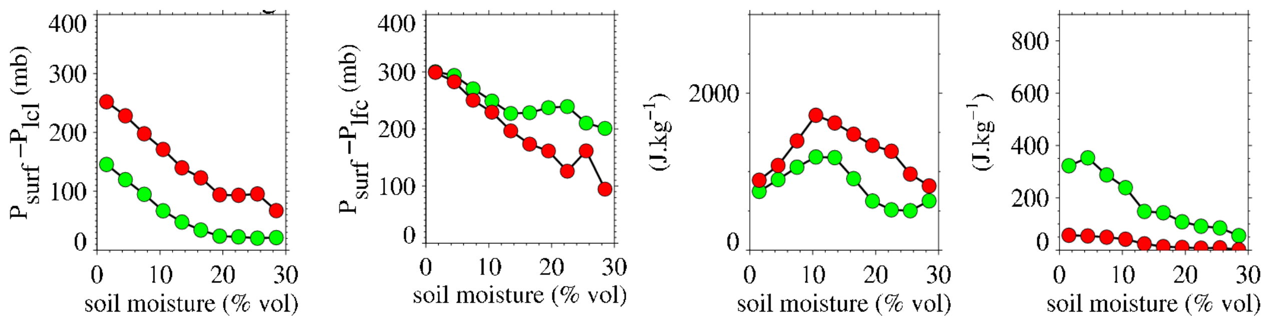

***Figure 5** : convective parameters and indexes as a function of surface soil moisture at 6h (green) and 12h (red), lifting condensation level (a proxi for cloud base height), level of free convection (middle-left), CAPE (middle-right) and CIN (right).The black lines joints the average values obtained by soil moisture range (see more in the appendix).*

Variations of CAPE with soil moisture are more complex. Indeed, there is hardly any correlation between soil moisture and CAPE. Overall, the higher values of CAPE are found at intermediate values of soil moisture. The lower values obtained for drier soils (resp. wetter soils) are associated with the strong reduction of the lower specific humidity (resp. temperature) (see also appendix). Nevertheless, it appears that the atmosphere is characterized by subtantial values of CAPE over the whole range of same sampled cases.
In the morning, the convective inhibition is particularly strong over the drier soils. It considerably decreases during daytime but remains higher than over wet soils.

From this analysis, we can conclude that the cases of initiation of deep convection can be organized as a function of coupled surface and atmospheric conditions. It is worth noticing that the datasets does not point to the emergence of isolated preferential regimes within the considered coupled spaces though. It rather points to a continuum with the advantage that it can be more robustly sampled.

REFERENCES

Boone, A., and Coauthors., 2009 : The AMMA Land Surface Model Intercomparison Project (ALMIP), Bull. Atmos. Meteor. Soc. doi : 10.1175/2009BAMS2786.1

F. Couvreux, C. Rio, F. Guichard, M. Lothon, G. Canut, D. Bouniol, A. Gounou, 2012: Initiation of daytime local convection in a semi-arid region analyzed with high-resolution simulations and AMMA observations. Quart. J. Roy. Meteor. Soc. 138, 56-71. doi: 10.1002/qj.903

Gounou, A., F. Guichard and F. Couvreux, 2012: Observations of Diurnal Cycles Over a West African Meridional Transect: Pre-Monsoon and Full-Monsoon Seasons. Boundary-Layer Meteorol., 144, 329-357. doi: 10.1007/s10546-012-9723-8

Guichard, F., and Coauthors, 2004: Modelling the diurnal cycle of deep precipitating convection over land with CRMs and SCMs. Quart. J. Roy. Meteor. Soc., 130, 3139-3172.

Lebel, T., and Coauthors, 2010: The AMMA field campaigns: multiscale and multidisciplinary observations in the West African region. Q.J.R. Meteorol. Soc., 136: 8–33. doi: 10.1002/qj.486

Machado, L. A. T., H. Laurent, and A. A. Lima, 2002 : Diurnal march of the convection observed during TRMM-WETAMC/LBA, J. Geophys. Res., 107(D20), 8064, doi:10.1029/2001JD000338

Taylor, C. M., A. Gounou, F. Guichard, P. P. Harris, R. J. Ellis, F. Couvreux and M. de Kauwe,2011: Frequency of Sahelian storm initiation enhanced over mesoscale soil-moisture patterns. Nature Geoscience, 4, 430-344, 10.1038/NGEO1173

Appendix

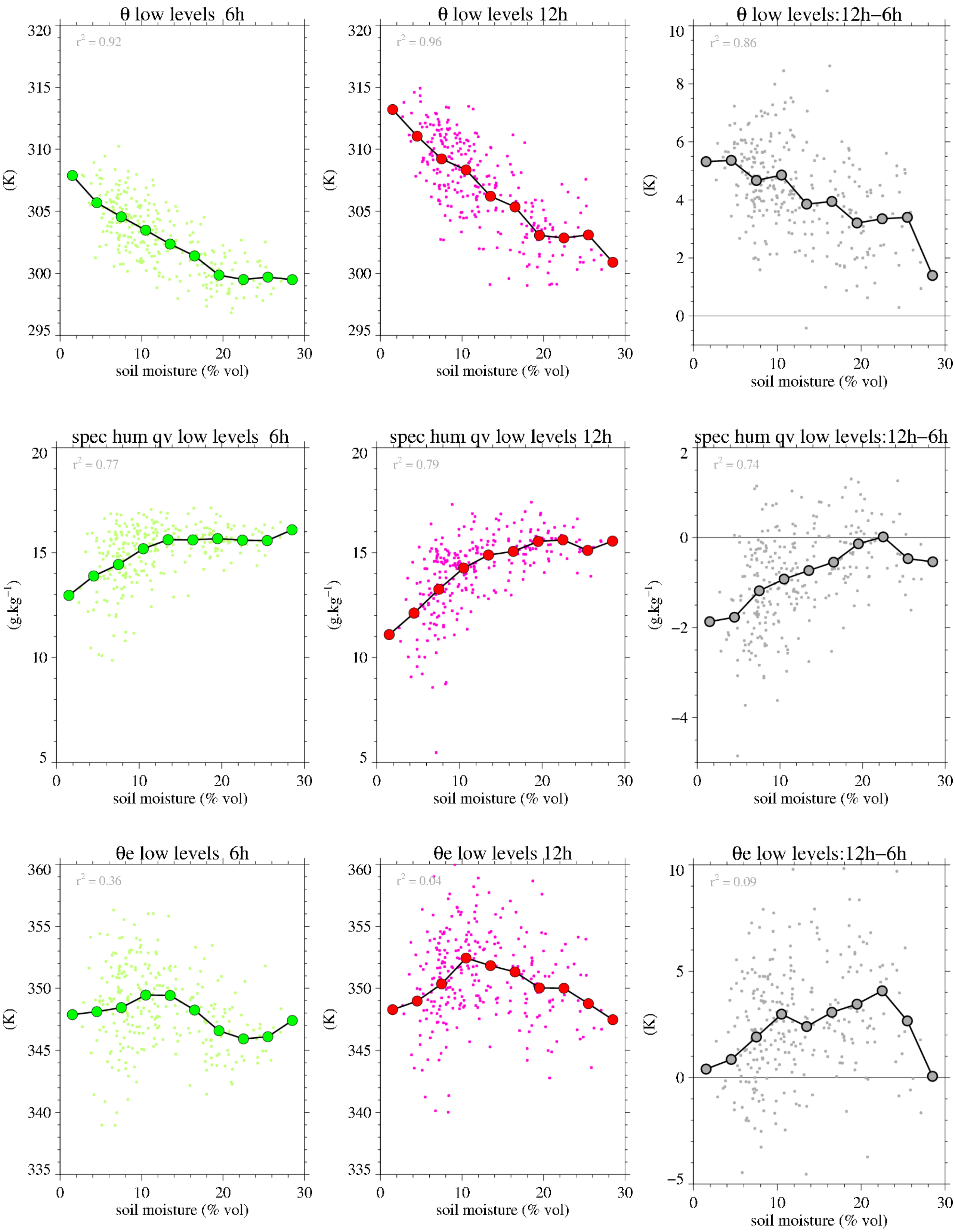

Figure A1 *: Thermodynamic of the low atmosphere (0-5000m AGL) as a function of surface soil moisture at 6h (left panel), 12 h (middle panel) and difference between 12h and 6h (right panel). Potential temperature, specific humidity and equivalent potential temperature (upper mid and lower panels). Each dot corresponds to one case and the black line joints the average values obtained by soil moisture range.*

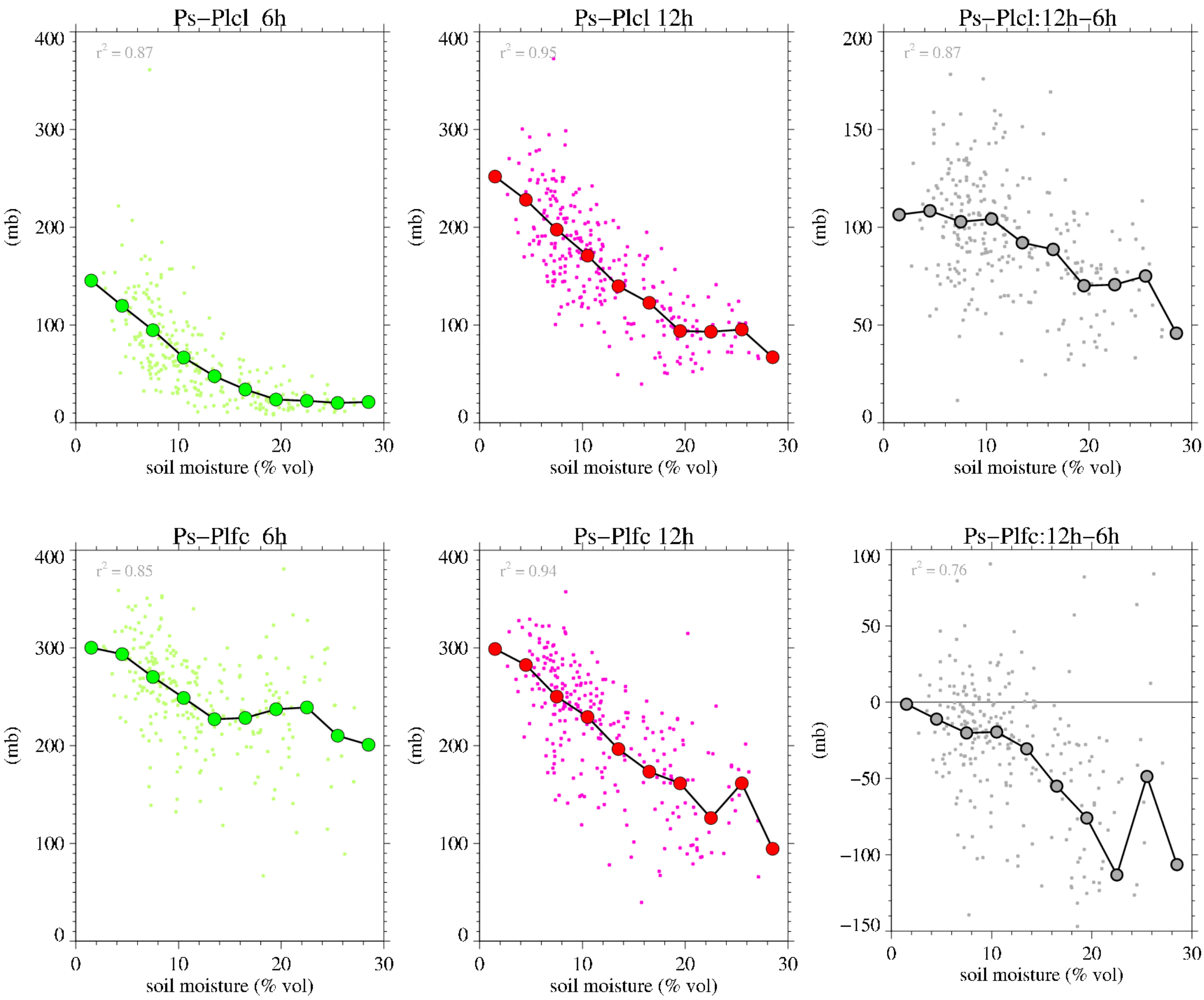

Figure A2 *: Same as figure A1 but for the lifting condensation level (upper panel) and the level of free convection (lowel panel).*

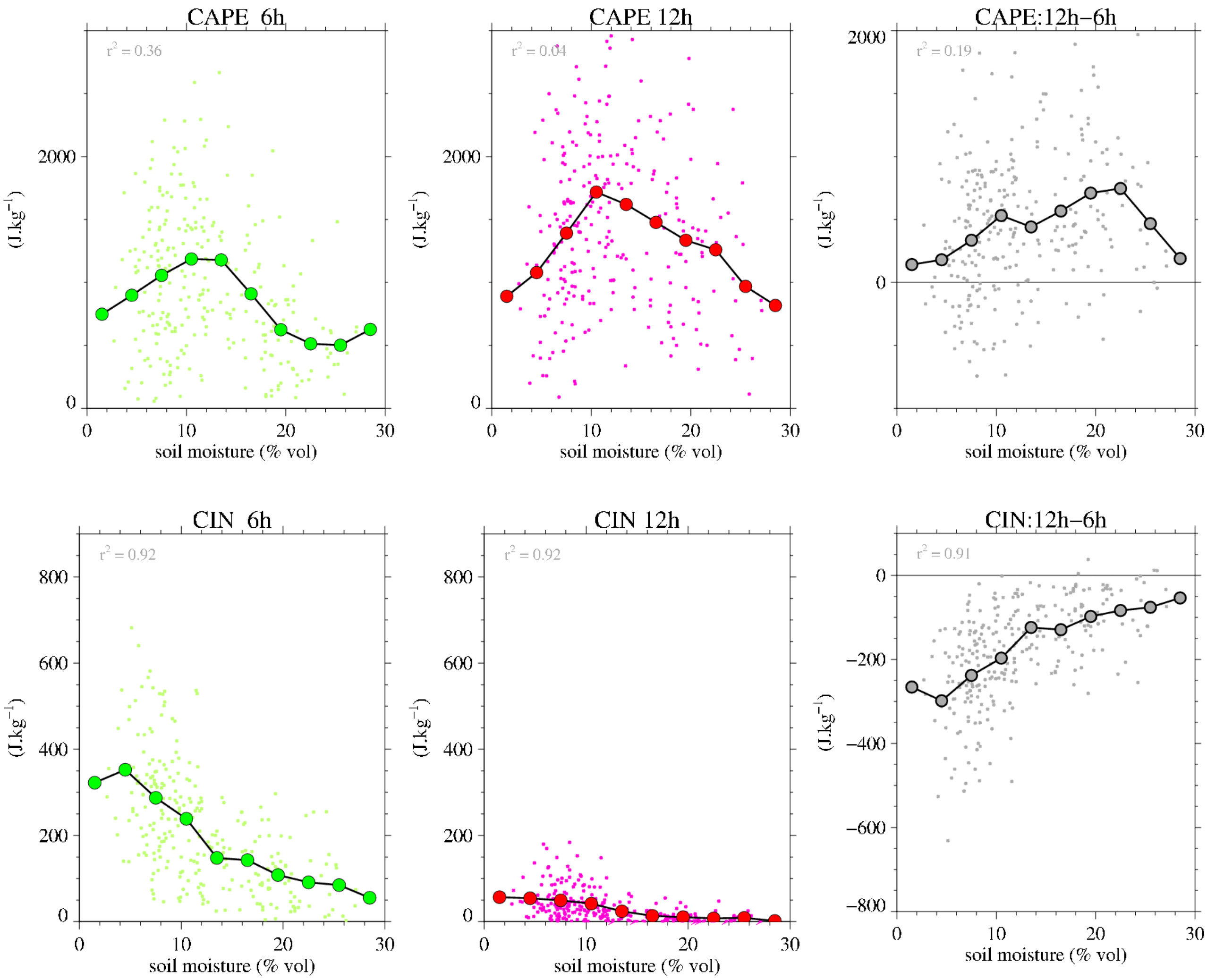

Figure A3 *: Same as figure A1 but for CAPE (upper panel) and CIN (lowel panel).*